Analytical Biochemistry **285,** 194–204 (2000)
doi:10.1006/abio.2000.4753, available online at http://www.idealibrary.com on IDEAL®

Quantitative Reverse Transcription–Polymerase Chain Reaction to Study mRNA Decay: Comparison of Endpoint and Real-Time Methods[1]

Thomas D. Schmittgen,*[,2] Brian A. Zakrajsek,* Alan G. Mills,† Vladimir Gorn,† Michael J. Singer,† and Michael W. Reed†

**Department of Pharmaceutical Sciences, College of Pharmacy, and the Cancer Prevention and Research Center, Washington State University, Pullman, Washington 99164-6534; and †Epoch Biosciences Inc., Redmond, Washington 98052*

Received December 10, 1999

Four quantitative reverse transcription–PCR (RT-PCR) methods were compared to evaluate the time course of mRNA formation and decay. Mouse fibroblasts (NIH 3T3) transfected with the human β-globin open reading frame/c-*myc* 3′-untranslated region chimeric gene under control of the c-*fos* promoter (fos-glo-myc) were used for serum-inducible transcription. The amount of fos-glo-myc mRNA, relative to β-actin, was measured by quantitative, RT-PCR at various times following the addition of serum to serum-starved fibroblasts transfected with the chimeric gene. Both endpoint (band densitometry and probe hybridization) and real-time (SYBR green and TaqMan) PCR methods were used to assay the identical cDNA. The real-time methods produced a 4- to 5-log dynamic range of amplification, while the dynamic range of the endpoint assays was 1-log. The real-time and probe hybridization assays produced a comparable level of sensitivity that was considerably greater than band densitometry. The coefficient of variation from 22 replicate PCR reactions was 14.2 and 24.0% for the SYBR green and TaqMan detection, respectively, and 44.9 and 45.1% for the band densitometry and probe hybridization assays, respectively. The rank order for the values of r^2 obtained from the linear regression of the first-order mRNA decay plots was SYBR green > TaqMan > probe hybridization > band densitometry. Real-time PCR is more precise and displays a greater dynamic range than endpoint PCR. Among the real-time methods, SYBR green and TaqMan assays produced comparable dynamic range and sensitivity while SYBR green detection was more precise and produced a more linear decay plot than TaqMan detection. © 2000 Academic Press

Key Words: **real-time PCR; endpoint PCR; mRNA stability; gene expression; TaqMan; SYBR green.**

Levels of expressed genes (i.e., mRNA) will change under a variety of conditions such as position within the cell cycle or upon exposure to drugs, hormones, cytokines, or other stimuli (1–4). The analysis of gene expression requires sensitive, precise, and reproducible measurement of specific mRNA sequences. The methods used to quantify mRNA include techniques based upon hybridization (e.g., Northern blotting, solution hybridization, and RNase protection assays) as well as the amplification of individual RNA molecules by combining reverse transcription and the polymerase chain reaction (RT-PCR).[3] The RT-PCR technique has been shown to correlate with the more traditional hybridization methods (5, 6). In addition, RT-PCR may be more sensitive because it exponentially amplifies small amounts of nucleic acid. This sensitivity enables the detection of rare mRNAs, mRNAs from small amounts of tissue, and mRNAs that are expressed in mixed cell populations.

A key factor in the quantitative ability of RT-PCR is measuring the product of the target gene within the

[1] Supported by Grants CA74375-01 (NIH) and IRG-119Q (American Cancer Society) to T.D.S.

[2] To whom reprint requests should be addressed. Fax: (509) 335-5902. E-mail: Schmittg@mail.wsu.edu.

[3] Abbreviations used: RT-PCR, reverse transcription polymerase chain reaction; CV, coefficient of variation; fos-glo-myc, chimeric gene composed of c-*fos* promoter, β-globin-coding sequence, and the c-*myc* 3′-untranslated region; MGB, minor groove binder ligand; D-MEM, Dulbecco's modified Eagle's medium.

0003-2697/00 $35.00

TABLE 1

Probe and Primer Sequences

Gene	RT-PCR assay	Forward primer	Reverse primer	Amplicon size (bp)	Probe[a]
Fos-glo-myc	Gel/probe	5′-Bio-GCTGCTGGTGGT CTACCCTT 3′	5′ CCCAGGAGCCTGAA GTTCTC 3′	231	5′ GAGCCTTCACCTTA GGGTTGCCC 3′
β-Actin	Gel/probe	5′-Bio-ACCAACTGGGAC GATATGGAGAAGA 3′	5′ TACGACCAGAGGCA TACAGGGACAA 3′	215	5′ GGTCATCTTTTCAC GGTTGGCCTTA 3′
Fos-glo-myc	SYBR/TaqMan	5′ GCTGCTGGTGGTCT ACCCTT 3′	5′ CCCAGGAGCCTGAA GTTCTC 3′	231	5′ FAM-CTGGACAACCT CAAG-MGB-3′
β-Actin	SYBR/TaqMan	5′ ACCAACTGGGACGA TATGGAGAAGA 3′	5′ TACGACCAGAGGCA TACAGGGACAA 3′	215	5′ FAM-CCCTCTGAACC CTAA-MGB-3′

Note. Bio, biotin; FAM, fluorescein; MGB, minor groove binder ligand, dihydrocyclopyrroloindole tripeptide.
[a] Probes were used in the probe hybridization and TaqMan assays only.

linear range of the amplification reaction. The amount of amplified target is directly proportional to the input amount of target only during this linear range of amplification. In traditional, or endpoint, RT-PCR analysis, the linear range of amplification is determined empirically by amplifying equivalent amounts of cDNA over different cycles of the PCR (7, 8) or by amplifying dilutions of cDNA over the same number of PCR cycles (9). The PCR product is detected following incorporation of a radiolabel (9), following staining an agarose gel with ethidium bromide (7, 8), or by probing the product post-PCR (10). The end result is that endpoint quantitative RT-PCR generates numerous samples resulting in a tedious and time-consuming assay.

Recent advances in quantitative RT-PCR technology include the development of real-time quantitative PCR (11). Real-time PCR incorporates specific technology to detect the PCR product following each cycle of the reaction. Several methods are available to detect the DNA generated by real-time PCR including dual-labeled fluorogenic hybridization probes (TaqMan probes) (11) and the SYBR green I minor groove DNA-binding dye (12). Real-time PCR allows sensitive detection of the DNA product, ensures detection during the linear range of amplification, eliminates the need for post-PCR analysis, and incorporates specialized software to simplify data analysis.

Our objective was to evaluate four quantitative RT-PCR assays that could be used to study mRNA formation and decay. An inducible gene transcription/decay assay was used for this purpose. Both endpoint (band densitometry and probe hybridization) and real-time (SYBR green and TaqMan) quantitative RT-PCR assays were evaluated. The criteria used to evaluate the assays include assay sensitivity, dynamic range, intraassay variation, and the linear regression analysis of the mRNA decay plots.

MATERIALS AND METHODS

Chemicals. Tissue culture reagents, Moloney murine leukemia virus reverse transcriptase, and random hexamers were purchased from Life Technologies (Gaithersburg, MD). The 4-methylumbelliferyl phosphate, hygromycin B, and RNase-free water were purchased from Sigma Chemical Co. (St Louis, MO). The RNeasy Mini RNA isolation kit was from Qiagen (Valencia, CA). Streptavidin-coated white microplates, anti-digoxygenin alkaline phosphatase, and RNase-free DNase I were from Boehringer-Mannheim (Indianapolis, IN). The Amplitaq Gold *Taq* DNA polymerase, MicroAmp 96-well plates, MicroAmp optical caps, and the SYBR green I PCR kits were purchased from PE Biosystems (Foster City, CA).

Tissue culture. NIH 3T3 fibroblasts stably transfected with the fos-glo-myc chimeric gene were generously provided by Dr. J. Ross (University of Wisconsin, Madison, WI). The chimeric fos-glo-myc gene consists of the β-globin-coding sequence fused in frame to a portion of the c-*myc* 3′-untranslated region. The chimeric gene was placed downstream from the serum-inducible c-*fos* promoter (13). The fos-glo-myc cells were cultured in a complete medium consisting of Dulbecco's modified Eagle's medium (D-MEM) supplemented with 10% calf serum, 100 U/ml penicillin, 100 μg/ml streptomycin, and 200 μg/ml hygromycin B. The cells were cultured at 37°C in a humidified environment of 5% CO_2/air.

PCR primers and probes. The sequences of the PCR primers and probes are listed in Table 1. For the probe hybridization analysis, the forward primers were labeled with biotin on the 5′ end and HPLC purified. For consistency, the 5′-biotinylated, forward primers were also used in the band densitometry assay. The dual-labeled fluorogenic hybridization probes (i.e., TaqMan probes) were labeled at the 5′ end with fluorescein and on the 3′ end with the quencher/minor groove binder

ligand dihydrocyclopyrroloindole tripeptide. The 3′ minor groove binder ligand allows use of shorter probes with better mismatch discrimination and lower fluorescent background (14). TaqMan probes with this 3′ quencher/minor groove binder structure are commercially available from PE Biosystems. The dual-labeled fluorogenic probes for real-time PCR were synthesized and purified as previously described (14). The fos-glo-myc and β-actin hybridization probes were purified by HPLC. The PCR primers and hybridization probes were synthesized and purified by Operon Technologies (Alameda, CA).

Serum stimulation experiments. The serum stimulation experiments were performed as previously reported (13) with the following modifications. Cells were plated in triplicate in six-well plates. Upon reaching 70% confluency, the cells were rinsed three times in warm phosphate buffered saline and cultured in D-MEM/penicillin/streptomycin and 0.5% dialyzed fetal bovine serum for 24 h. Following the starvation period, cells were induced by adding 15% dialyzed fetal bovine serum. At 0, 0.5, 1, 1.5, 2, 3, 4, 6, and 8 h following the addition of serum, the medium was removed and the cells were lysed in 350 μl of buffer RLT (Qiagen). Cell lysis was performed at room temperature. The cell lysates were immediately frozen in a dry ice/ethanol slurry and stored at −80°C.

RNA extraction and reverse transcription. Total cellular RNA was isolated from the fibroblasts using the RNeasy Mini, RNA isolation kit per the manufacturer's protocol. Total RNA was eluted from the matrix with 35 μl of RNase-free water. Residual genomic DNA was removed by incubating the RNA solution with 15 units of RNase-free DNase I in 2 mM $MgCl_2$ for 10 min at 37°C followed by 5 min at 90°C to inactivate the DNase. Twenty-five microliters of the DNase-treated RNA solution was used in a reaction containing 50 mM Tris–HCl (pH 8.3), 10 mM dithiothreitol, 0.0225 A_{260} units of random hexamers, 3.5 μg bovine serum albumin, 3 mM $MgCl_2$, 0.5 mM deoxynucleotide triphosphates, 30 units of RNAguard RNase inhibitor (Promega, Madison, WI), 500 units of Moloney murine leukemia virus reverse transcriptase, and RNase-free water to 50 μl. The reverse transcription reactions were not normalized to contain equivalent amounts of total RNA. The reactions were incubated at 26°C for 10 min and then at 42°C for 45 min followed by a 3-min incubation at 90°C to denature RNA secondary structure. An additional 300 units of reverse transcriptase was added and the reactions were incubated for 45 min at 42°C followed by 75°C for 10 min to inactivate the reverse transcriptase. The cDNA samples were aliquoted and stored at −80°C. The identical cDNA samples were used throughout the study.

Real-time PCR: SYBR green detection. The PCR was performed in the PE Biosystems GeneAmp 5700 sequence detection system using the SYBR green I PCR kit as recommended by the manufacturer. Each reaction contained 2.5 μl of the 10× SYBR green buffer; 200 nM dATP, dGTP, and dCTP; 400 nM dUTP; 2 mM $MgCl_2$; 0.25 units of uracil *N*-glycosylase, 0.625 units of Amplitaq Gold DNA polymerase; 250 nM forward and reverse primers; 5 μl of a 1:10 dilution of the cDNA; and water to 25 μl. The reactions were performed in MicroAmp 96-well plate capped with MicroAmp optical caps. The reactions were incubated at 50°C for 2 min to activate the uracil *N*′-glycosylase and then for 10 min at 95°C to inactivate the uracil *N*′-glycosylase and activate the Amplitaq Gold polymerase followed by 55 cycles of 15 s at 95°C, 30 s at 55°C, and 30 s 72°C. The PCR reactions were subjected to a heat dissociation protocol present in the PE Biosystems 5700 software. Following the final cycle of the PCR, the reactions were heat denatured over a 35°C temperature gradient at 0.03°C/s from 60 to 95°C.

Real-time PCR: TaqMan detection. Reactions for the real-time PCR using TaqMan detection consisted of 2.5 μl of a 10× TaqMan buffer A (PE Biosystems); 200 nM dATP, dGTP, and dCTP; 400 nM dUTP; 4.5 mM $MgCl_2$; 0.25 units of uracil *N*-glycosylase; 0.625 units of Amplitaq Gold DNA polymerase; 250 nM forward and reverse primers; 250 nM dual-labeled fluorogenic hybridization probe; 5 μl of a 1:10 dilution of the cDNA; and water to 25 μl. Real-time PCR was performed identically to that described for SYBR green except that the heat denaturation protocol was omitted.

Real-time PCR: Data analysis. The data generated from both SYBR green and TaqMan chemistries were analyzed in a similar manner. The real-time PCR data were plotted as the ΔR_n fluorescence signal versus the cycle number. The PE Biosystems 5700 sequence detection system software calculates the ΔR_n using the equation $\Delta R_n = (R_n^+) - (R_n^-)$, where R_n^+ is the fluorescence signal of the product at any given time and R_n^- is the fluorescence signal of the baseline emission during cycles 6 to 15. An arbitrary threshold was set at the midpoint of the log ΔR_n versus cycle number plot. The C_t value is defined as the cycle number at which the ΔR_n crosses this threshold. The fold change in fos-glo-myc cDNA (target gene) relative to the β-actin endogenous control was determined by:

$$\text{Fold change} = 2^{-\Delta\Delta C_t}, \qquad [1]$$

where $\Delta\Delta C_t = (C_{t\text{Target}} - C_{t\text{Actin}})_{\text{Time}\,x} - (C_{t\text{Target}} - C_{t\text{Actin}})_{\text{Time}\,0}$. Time x is any time point and time 0 represents the 1× expression of each gene under conditions of serum starvation. Relative quantification of gene expression using the $2^{-\Delta\Delta C_t}$ method correlated

with the absolute gene quantification obtained using standard curves (16).

Endpoint PCR. PCR reactions for the probe hybridization assay consisted of a 1× Amplitaq Gold buffer, 2 mM $MgCl_2$, 200 nM each dNTP, 250 nM biotinylated forward and reverse primer, 5 μl of the cDNA diluted in water, 0.625 U of Amplitaq Gold *Taq* polymerase, and water to 25 μl. The PCR conditions for the band densitometry analysis were identical to the probe hybridization assay except that the reactions were scaled up to 100 μl. The biotinylated, forward primer was required for the probe hybridization assay but was also used in the band densitometry assay for consistency. The reactions were incubated for 10 min at 95°C to activate the Amplitaq Gold polymerase, followed by 30 cycles of 15 s at 95°C, 30 s at 55°C, and 30 s at 72°C. To standardize the instrumentation for the study, the endpoint PCR reactions were performed in the PE Biosystems GeneAmp 5700 Sequence Detection System thermocycler.

Endpoint PCR: Ethidium bromide-stained gel detection. The 100 μl reactions were concentrated to approximately 20 μl in a Speed Vac concentrator (Savant Instruments, Farmingdale, NY) to facilitate loading the gel. This increased the detection limit of the assay. The concentrated reactions were loaded onto a 2.2% agarose/TAE gel containing 0.5 μg/ml ethidium bromide and run for 1.5 h at 2.5 V/cm. The gel was photographed on an UV transilluminator with Type 665 positive/negative Polaroid film. The negative was digitized with a Hewlett Packard Model 4C scanner and the amount of DNA in the fos-glo-myc and β-actin bands was quantified using Scanalytics RFLP Scan software.

Endpoint PCR: Probe detection in microtiter plates. Five microliters of the PCR product was analyzed by probe hybridization in microtiter plates as previously described with a few modifications (10). The antisense hybridization probes were 3′ end-labeled with digoxygenin using the digoxygenin labeling kit (Boehringer-Mannheim). The digoxygenin-labeled probes were diluted in hybribization solution at 5 pmol/μl, and 200 μl was added to each well and incubated at 60°C for 1 h. The wells were rinsed three times with a posthybridization wash solution (0.5× standard saline citrate, 0.1% Tween 20), incubated in 200 μl of posthybridization wash solution at 60°C followed by three additional washings of posthybridization wash solution. Anti-digoxygenin alkaline phosphatase (150 U/200 μl) was diluted to 0.2 μl/ml in PBS/Boehringer-Mannheim blocking reagent and 200 μl of this solution was added to each well and incubated at 37°C for 1 h. The strips were washed six times in wash buffer. Two-hundred microliters of 0.8 mM 4-methylumbelliferyl phosphate in 50 mM boric acid, 50 mM KCl, 0.1 M $MgCl_2$, pH 10, was added for 1 h at 37°C. The reactions were quenched with 50 μl of 3 M K_2HPO_4 and the fluorescence was detected in a CytoFluor series 4000 multiwell plate reader (PerSeptive Biosystems, Farmington, MA), excitation 360 nm and emission 440 nm.

Endpoint PCR to measure mRNA formation and decay. The linear range of amplification for the endpoint assays was determined by amplifying serial dilutions of cDNA from samples that contained the highest expression of fos-glo-myc and β-actin. To determine which cDNA samples contained the highest expression of each gene, the cDNA samples collected during the serum stimulation study were quantified using the SYBR green real-time assay. Samples of cDNA containing the highest expression of fos-glo-myc and β-actin were chosen, serially diluted, and amplified by 30 cycles of the PCR using primers for fos-glo-myc or β-actin. The products were detected using the band densitometry or probe hybridization assays. A volume of cDNA that was within the linear range was selected and this volume was amplified for each point in the time course study. The fold change in fos-glo-myc mRNA was presented as:

$$\text{Fold change} = \frac{\left(\frac{\text{Signal}_{\text{Target}}}{\text{Signal}_{\text{Actin}}}\right)_{\text{Time } X}}{\left(\frac{\text{Signal}_{\text{Target}}}{\text{Signal}_{\text{Actin}}}\right)_{\text{Time 0}}}, \qquad [2]$$

where the signal represents the band density or fluorescence signal emitted for the band densitometry or probe hybridization assays, respectively. The background emission from a no template control reaction was subtracted from the density or fluorescence signal at each time point. Time x and time 0 are the same as that described in Eq. [1].

Statistics. Linear regression analysis was performed on the individual samples assayed at 1, 1.5, 2, 3, and 4 h following serum stimulation. Values for the first-order rate constant for mRNA decay, r^2, and standard error of the estimates were calculated from the linear regression analysis using Microsoft Excel (Microsoft Corporation, Seattle, WA).

RESULTS

Real-Time PCR Analysis

Figure 1 illustrates a typical plot of data generated by real-time PCR using SYBR green detection. Similar plots were generated using TaqMan detection (not shown). The PCR signal is initially below the limit of detection and increases with cycle number to cross a threshold. The threshold was set to the midlinear portion of the log ΔR_n versus cycle plot (Fig. 1A, inset).

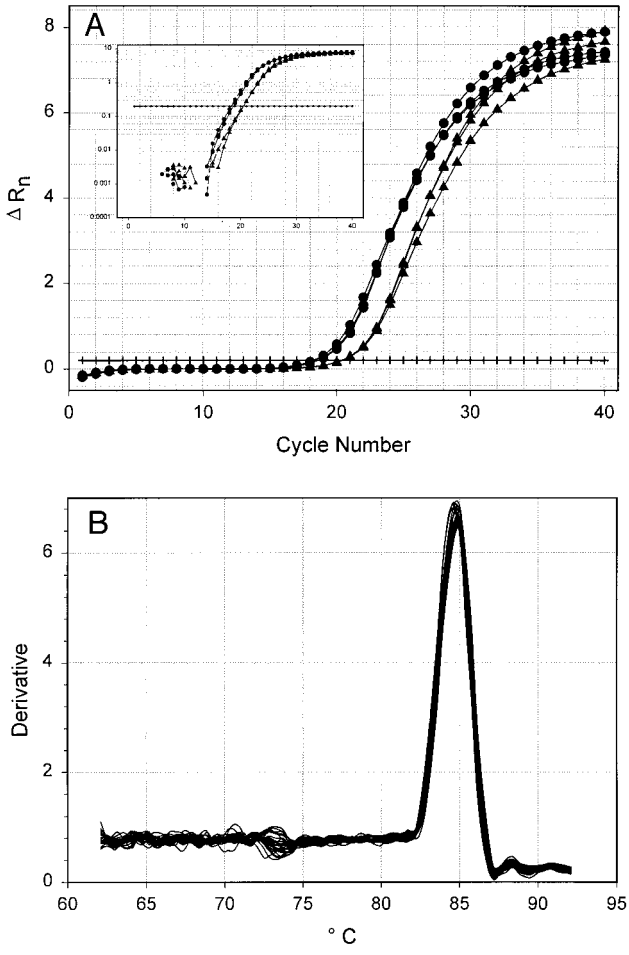

FIG. 1. Real-time PCR analysis of cellular mRNA levels. (A). Plot of the ΔR_n versus cycle number obtained from the SYBR green detection of fos-glo-myc mRNA. Triplicate samples of cDNA obtained from three different RNA isolations of mouse fibroblasts stimulated with serum for 1.5 (circles) and 8 h (triangles) ($N = 3$). The line represents the threshold arbitrarily set in the middle of the log ΔR_n plot (inset). (B). Heat dissociation protocol. The entire series of cDNAs from the time course study ($N = 27$) was amplified by 40 cycles of the PCR using primers for fos-glo-myc and SYBR green detection. Following the final PCR cycle the samples were subjected to a heat dissociation protocol over the indicated temperature range.

The cycle number at which the signal crosses the threshold is defined as C_t. Input cDNA copy number and C_t are inversely related; a sample that contains more copies of template will cross the threshold at an earlier cycle compared to one containing fewer copies of template. For example, the sample exposed to serum for 1.5 h ($C_t = 19$) had a higher input copy number than the sample exposed to serum for 8 h, $C_t = 20.5$ (Fig. 1A).

Since SYBR green I indiscriminately binds to double-stranded DNA, other products in the PCR such as primer dimers may be detected along with the target gene (15). To verify that the SYBR green dye detected only one PCR product, the samples were subjected to the heat dissociation protocol following the final cycle of the PCR. Heat dissociation of oligonucleotides detects differences in melting temperature (e.g., GC/AT ratio) and will produce a single dissociation peak for each oligonucleotide within a 2°C difference in melting temperature (17). Dissociation of the PCR reactions consistently produced a single peak for fos-glo-myc (Fig. 1B) and β-actin (not shown), demonstrating the presence of only one product in the reaction. The presence of a single product was further verified by gel electrophoresis (not shown).

Triplicate cDNAs from each time point following serum induction were amplified using primers for fos-glo-myc or β-actin and detected with SYBR green. The amount of fos-glo-myc and β-actin from each sample was transformed equal to 2^{-C_t} in order to convert C_t (logarithmic value) to a linear value. The data were presented as the fold change in mRNA expression relative to the amount present at time zero and were not normalized to an internal control gene. The level of fos-glo-myc mRNA immediately increased following the addition of serum, peaked at 60 min, and then declined (Fig. 2). This pattern of fos-glo-myc mRNA induction and decay follows that previously reported by Herrick and Ross who measured mRNA levels in the same cell line by Northern blotting (13). Serum appeared to influence the expression of β-actin; a steady

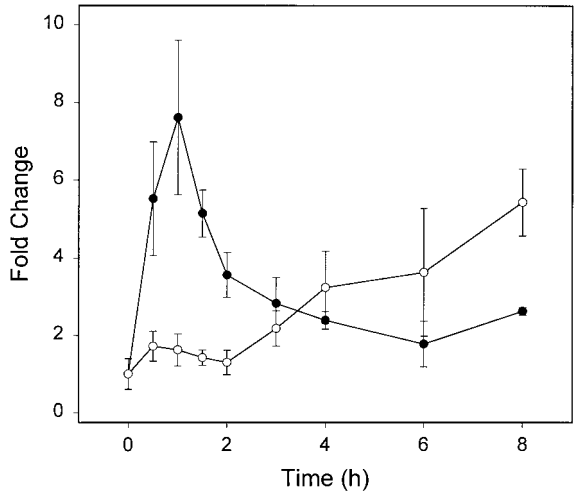

FIG. 2. Induction and decay of the fos-glo-myc and β-actin mRNA; real-time PCR analysis. Mouse fibroblasts transfected with the chimeric fos-glo-myc gene were serum starved for 24 h and induced with 15% serum over 8 h. Total RNA was isolated from the cells at each time point and converted to cDNA. Samples of cDNA (0.1 μl) were amplified using real-time quantitative PCR and SYBR green detection as described under Materials and Methods. Presented is the fold change in the expression of fos-glo-myc (●) and β-actin (○) following addition of serum. The fold change in mRNA expression is presented as 2^{-Ct} and was not normalized to an internal control gene. Mean ± SD ($N = 3$).

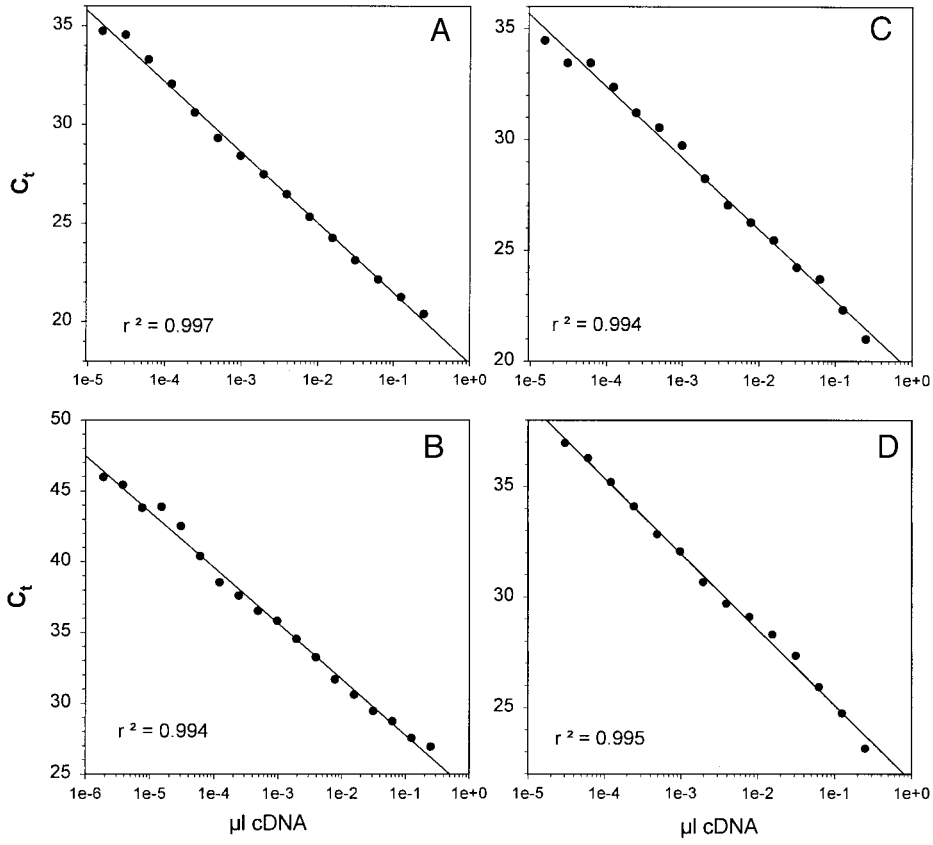

FIG. 3. Sensitivity and dynamic range of real-time, quantitative PCR. Serial dilutions of cDNA (0.25 μl to 1.2×10^{-7} μl) from fibroblasts exposed to serum for 1 h were amplified using real-time, quantitative PCR. Diluted cDNA was amplified and detected by SYBR green using primers for fos-glo-myc (A) or β-actin (B) or using TaqMan probes and primers for fos-glo-myc (C) or β-actin (D). The dynamic range for each assay is presented. The r^2 was determined using least-squares linear regression ($N = 1$).

increase in the β-actin expression was observed over the 8 h of serum stimulation (Fig. 2).

Sensitivity and Dynamic Range of the RT-PCR Assays

The sensitivity and dynamic range of the quantitative RT-PCR assays were determined by amplifying serial dilutions of cDNA. For the endpoint assays, the lower limit of detection was defined as the point when the signal intensity was similar to that of the no template control. The minimal detectable limit of the real-time assays was defined as the point at which the relationship between C_t and the cDNA became nonlinear. Serial dilutions of cDNA (0.25 μl to 1.2×10^{-7} μl) from fibroblasts exposed to serum for 1 h were amplified using primers for fos-glo-myc or β-actin and the products were detected using SYBR green or TaqMan probes. The relationship between C_t and the volume of cDNA was linear between 0.25 and 1.5×10^{-5} μl for fos-glo-myc (Fig. 3). Amplification of β-actin was linear between 0.25 and 2×10^{-6} μl and 0.25 and 3×10^{-5} μl when detected by SYBR green and TaqMan, respectively. The r^2 from the linear regression was >0.99 for the amplification of both genes using either real-time assay (Fig. 3). A strong linear relationship over a 4-log dynamic range exists for both SYBR green and TaqMan detection.

The dynamic range of the endpoint assays was determined by amplifying serial dilutions of cDNA from fibroblasts exposed to serum for 1 (fos-glo-myc primers) and 8 h (β-actin primers). One and 8 h were chosen because these samples contained the greatest amount of fos-glo-myc and β-actin, respectively (Fig. 2). Dilutions of cDNA (0.25 to 3.0×10^{-5} μl) were amplified by 30 cycles of the PCR. The PCR products were resolved by electrophoresis and the amount of DNA present in the gel was determined by band densitometry. The band densitometry assay was linear between 3.1×10^{-2} and 9.8×10^{-4} μl of cDNA for fos-glo-myc ($r^2 = 0.993$) and between 3.91×10^{-3} and 2.4×10^{-4} for β-actin ($r^2 = 0.986$, Fig. 4). The minimal detectable amount of cDNA using the band densitometry assay was 9.8×10^{-4} μl for fos-glo-myc and 2.4×10^{-4} for β-actin. A volume of cDNA that was within the linear

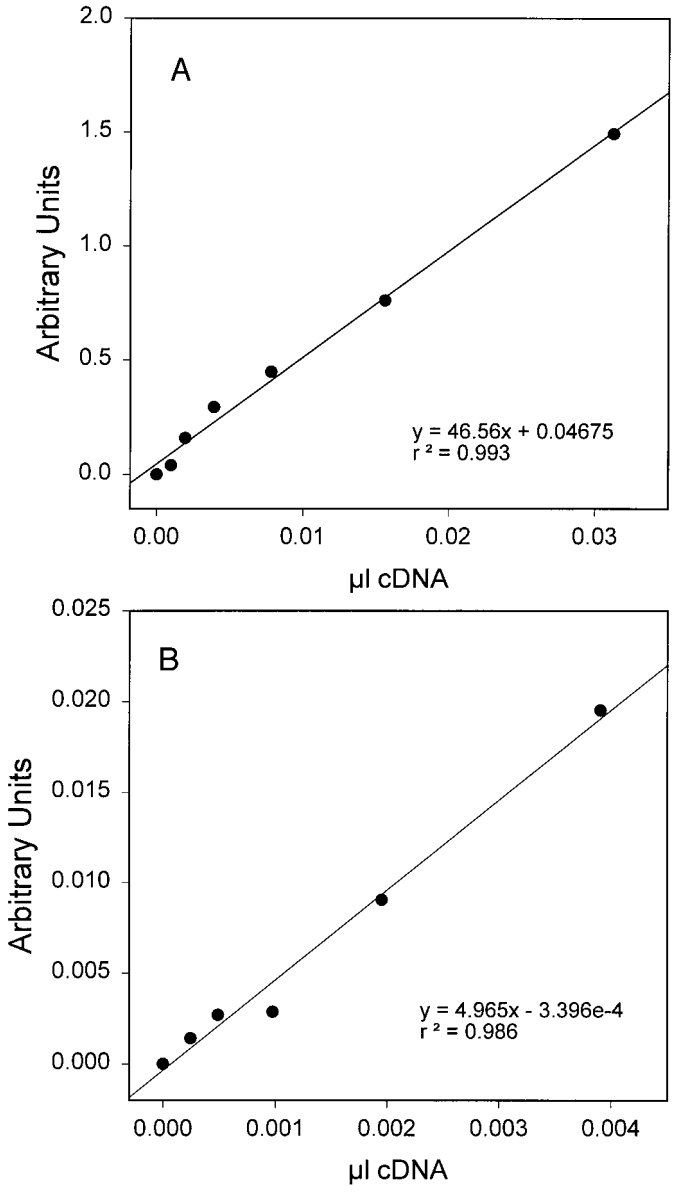

FIG. 4. Linear range of amplification; band densitometry detection. Serial dilutions of cDNA (0.25 to 1.5 $\times$ 10^{-5}) obtained from serum-stimulated fibroblasts were amplified by 30 cycles of the PCR. The amount of product present in each reaction was determined from the ethidium bromide-stained agarose gel as described under Materials and Methods. The linear range of amplification is shown for a cDNA sample (1 h serum exposure) amplified with primers for fos-glo-myc (A) and a cDNA sample (8 h serum exposure) amplified using primers for β-actin (B) ($N = 1$).

range for both fos-glo-myc and β-actin was selected (3.9×10^{-3} μl) and was used in the subsequent amplification of all 27 samples in the time course study.

The dynamic range of the hybridization assay was determined by amplifying serial dilutions of cDNA (0.125 to 3.8 $\times$ 10^{-6}) using primers for fos-glo-myc (1 h sample) and β-actin (8 h sample). The probe hybridization assay was linear between 2.4 $\times$ 10^{-4} and 1.5 $\times$ 10^{-5} μl of cDNA ($r^2 = 0.989$) for fos-glo-myc and between 5 $\times$ 10^{-4} and 1.5 $\times$ 10^{-5} μl for β-actin ($r^2 = 0.995$, Fig. 5). The minimal detectable limit for the probe hybridization assay for both genes was 1.5 $\times$ 10^{-5} μl of cDNA. A volume of cDNA that was within the linear range for both fos-glo-myc and β-actin was selected (2.4 $\times$ 10^{-4} μl) and was used in the subsequent

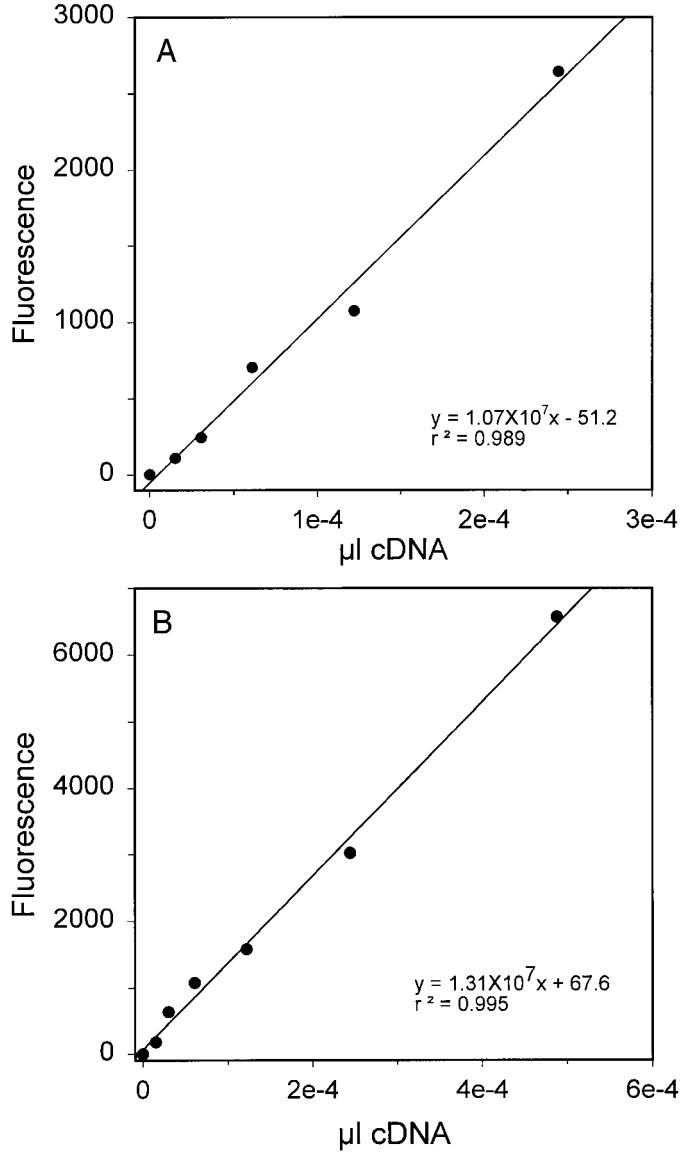

FIG. 5. Linear range of amplification; probe hybridization detection. Serial dilutions of cDNA (0.125 to 3.8 $\times$ 10^{-6} μl) obtained from serum-stimulated fibroblasts were amplified by 30 cycles of the PCR. The amount of product present in each reaction was determined by the probe hybridization assay described under Materials and Methods. The linear range of amplification is shown for a cDNA sample (1 h serum exposure) amplified with primers for fos-glo-myc (A) and a cDNA sample (8 h serum exposure) amplified using primers for β-actin (B) ($N = 1$).

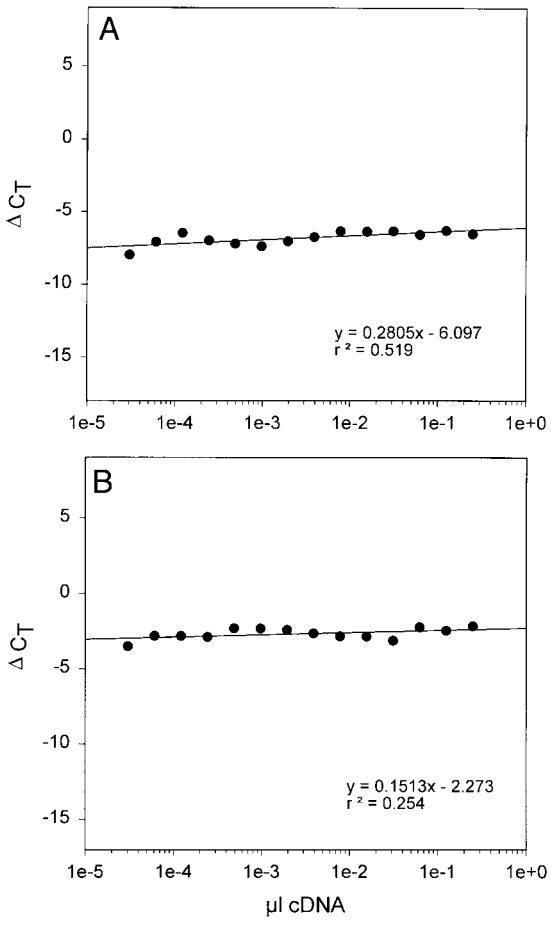

FIG. 6. Efficiency of fos-glo-myc and β-actin amplification by real-time PCR. The efficiency of amplification of fos-glo-myc and β-actin was examined by amplifying cDNA from fibroblasts exposed to serum for 1 h. Serial dilutions of cDNA (0.25 to 1.2×10^{-7} μl) was amplified by real-time PCR using gene-specific primers and was detected by SYBR green (A) or TaqMan probes (B). The ΔC_t ($C_{tTarget} - C_{tActin}$) was calculated for each volume of cDNA that was amplified. The data were fit using least-squares linear regression analysis ($N = 1$).

amplification of all 27 samples in the time course study.

Validation of $2^{-\Delta\Delta C_t}$ Method for Real-Time, Quantitative PCR

For the real-time assays, the fold change in fos-glo-myc mRNA was determined using the $2^{-\Delta\Delta C_t}$ method as described under Materials and Methods. The $2^{-\Delta\Delta C_t}$ method assumes that the amplification efficiency of the target gene and the internal control gene are the same. Amplicon efficiency is tested by plotting the log of the input template versus the ΔC_t; a slope of approximately zero demonstrates that the efficiencies are equal. To validate the use of the $2^{-\Delta\Delta C_t}$ method in the present study, the ΔC_t ($C_{tTarget} - C_{tActin}$) was calculated at each input cDNA from the data presented in Fig. 3. The linear regression from both the SYBR green and TaqMan plots reveal a slope of approximately zero (Fig. 6). Thus, the amplification efficiencies of both amplicons are similar and the fold change in fos-glo-myc gene expression may be presented as $2^{-\Delta\Delta C_t}$ for both SYBR green and TaqMan detection.

Precision of Real-Time and Endpoint Assays

The intraassay precision of the four quantitative RT-PCR assays was determined by quantifying the relative amount of fos-glo-myc mRNA from 22 replicate PCRs. Samples of cDNA exposed to serum for 0 and 1 h were diluted to 2.4×10^{-4} μl and were amplified by the probe hybridization assay. Other samples of cDNA exposed to serum for 0 and 1 h were diluted to 3.9×10^{-3} μl and were assayed using the band densitometry and real-time PCR assays. The samples were diluted to the appropriate volumes to ensure linearity for the endpoint assays. The relative amount of fos-glo-myc to β-actin was calculated as described under Materials and Methods. The mean fold change in fos-glo-myc expression over 1 h of serum stimulation was about threefold when assayed by the real-time methods and band densitometry and fivefold when assayed by probe hybridization (Table 2). The endpoint assays produced a comparable level of variation that was much greater than the variation in the real-time methods. The CV of the band densitometry and probe hybridization assays were 44.9 and 45.1%, respectively, while the CV of the SYBR green and TaqMan assays were 14.2 and 24.0%, respectively (Table 2).

Quantitative RT-PCR Analysis of mRNA Induction and Decay

The relative amount of fos-glo-myc to β-actin mRNA at each time point following serum stimulation was

TABLE 2

Intraassay Precision among Quantitative RT-PCR Assays

RT-PCR assay	Mean fold change in fos-glo-myc expression	SD	CV (%)	*N*
Band densitometry	2.70	1.21	44.9	22
Probe hybridization	4.93	2.22	45.1	22
SYBR green	2.70	0.384	14.2	22
TaqMan	3.44	0.824	24.0	22

Note. 22 replicate PCRs were performed on the identical cDNA synthesized from fibroblasts exposed to serum for 0 or 1 h. The cDNA was amplified using primers for fos-glo-myc or β-actin and the amount of PCR product was detected using the four quantitative PCR assays listed below. The relative amount of fos-glo-myc to β-actin was calculated as described under Materials and Methods. The mean fold change in fos-glo-myc mRNA expression over 1 h of serum-stimulation is reported.

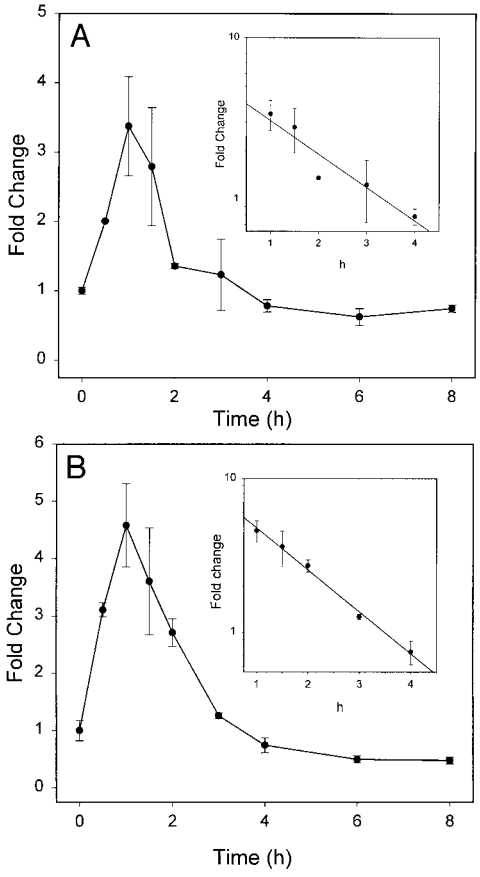

FIG. 7. Comparison of mRNA induction and decay by endpoint and real-time RT-PCR. Serum-starved fibroblasts transfected with the inducible fos-glo-myc gene were stimulated with serum over 8 h. Total RNA was extracted from the cells at various times and converted to cDNA and the identical cDNA was quantified using both RT-PCR assays. The relative amount of fos-glo-myc to β-actin was determined using a gel electrophoresis end point assay (A) or by real-time quantitative PCR with SYBR green detection (B). Mean $\pm$ SD ($N = 3$). First-order decay plots of fos-glo-myc mRNA (insets).

quantified using the real-time and endpoint RT-PCR assays. The fold change in fos-glo-myc expression was plotted as a function of the serum exposure time for the band densitometry and SYBR green detection (Fig. 7) and for the probe hybridization and TaqMan assays (not shown). The first-order rate constants for mRNA decay, r^2, and the standard error of the estimates were calculated from the linear regression (Table 3). The values for mRNA half-life determined by quantitative RT-PCR were similar to the 1-h half-life reported by Herrick and Ross who measured mRNA levels in the same cell line by Northern blotting (13). The rank order for the values of r^2 was SYBR green > TaqMan > probe hybridization > band densitometry while the rank order for the standard error of the estimates was SYBR green < TaqMan < band densitometry < probe hybridization.

DISCUSSION

Prior studies have compared real-time and endpoint quantitative PCR methods by examining the variation and sensitivity of detection obtained from amplifying DNA from clinical specimens (18, 19). The intent of this study was to evaluate the data generated from end point and real-time quantitative PCR by amplifying cDNA synthesized from mRNA. Mouse fibroblasts transfected with the fos-glo-myc chimeric gene were used for this purpose (13). This experimental system was chosen because transcription of the target gene is easily initiated by adding serum to serum-starved fibroblasts transfected with the chimeric gene. Moreover, since the gene contains the adenylate and uridylate-rich destabilizing sequence, mRNA decay may be followed over a relatively short period of time after stimulation with serum. Since cDNA is stable when stored at -80°C, the identical cDNA was analyzed using the four quantitative PCR assays.

The levels of expressed genes may be measured by relative or absolute quantitative RT-PCR. Absolute quantitation relates the PCR signal to input copy number using a standard curve (16), while relative quantification measures the relative change in mRNA expression. Relative quantitation was used here to study mRNA decay because the mRNA copy number does not need to be known in order to collect kinetic data. Relative quantitation is easier to perform than absolute quantitation because standard curves are not necessary.

The minimum volume of cDNA in which fos-glo-myc was detectable was 1.5×10^{-5} μl for both real-time and probe hybridization assays. By comparison, the lower level of sensitivity of fos-glo-myc by band densitometry was 9.8×10^{-4} μl. Thus, the real-time and probe hy-

TABLE 3

Linear Regression Analysis of mRNA Decay Obtained from Four Quantitative RT-PCR Assays

RT-PCR assay	k (h^{-1})	mRNA half-life (h)	r^2	Standard error
Band densitometry	0.476	1.46	0.777	0.295
Probe hybridization	0.802	0.864	0.858	0.378
SYBR green	0.627	1.11	0.957	0.153
TaqMan	0.472	1.47	0.903	0.179

Note. Fibroblasts transfected with the inducible fos-glo-myc gene were serum-starved and induced with serum for 8 h. Triplicate samples were collected at various times following serum stimulation and cDNA was prepared as described under Materials and Methods. The relative amount of fos-glo-myc was determined from the identical cDNA using the four quantitative PCR assays shown below. The first-order rate constants for fos-glo-myc mRNA degradation (k), r^2, and standard error were obtained from the linear regression analysis of the mRNA decay plots.

bridization assays were 65-fold more sensitive in detecting fos-glo-myc than band densitometry. The endpoint assays produced a comparable level of intraassay variation that was greater than the real-time methods (Table 2). Since the probe hybridization assay was more sensitive than band densitometry detection, yet both assays produced similar variation, we conclude that assay sensitivity was not responsible for the reduced precision in endpoint detection compared to real-time PCR. The replicate experiment presented in Table 2 was performed by pipetting a master mix of cDNA and PCR reagents into individual reaction tubes. Since master mixes were used in both the real-time and endpoint assays, the increased variation observed with endpoint detection was not due to pipetting errors. One explanation for the increased variation of the endpoint assays is the post-PCR manipulations (e.g., additional pipetting steps, washes, loading gels) that were necessary to detect the PCR product.

The CV from 22 replicate PCRs were 14.2 and 24.0% for the SYBR green and TaqMan assays, respectively (Table 2). The CV of 40 replicate reactions using TaqMan detection was reported as 1.6 % (18). Other studies have reported the CV from TaqMan detection to be around 1% (11, 16). In each of the previously reported studies, the CV was calculated from the raw C_t values. In the present study, the fold change in mRNA expression was calculated from the formula $2^{-\Delta\Delta C_t}$. This calculation transforms the logarithmic C_t data to a linear value. To determine the error of data that is not presented as the fold change in expression, we suggest converting the data from logarithmic to linear using the expression 2^{-C_t}. To emphasize this point, the mean ± SD (CV) of 22 replicate SYBR green PCRs of the fos-glo-myc gene (1 h serum exposure) was recalculated. When calculated from the raw C_t, the mean was 25.0 ± 0.182 (CV = 0.730%); however, when the individual C_t values were converted to the linear form equal to 2^{-C_t}, the mean was $3.07 \times 10^{-8} \pm 4.04 \times 10^{-9}$ (CV = 13.2 %). Presentation of statistical data calculated from the raw C_t values falsely represents the error and should be avoided.

The linear range of amplification for each cDNA sample in the time course study was not determined for the endpoint assays. Instead, the linear range was established in samples that contained the highest expression of the target and internal control genes. For simplicity, real-time PCR was used to determine which samples had the highest level of gene expression (Fig. 2). A volume of cDNA that was within the linear range was selected and this volume of cDNA was amplified in each of the samples in the study. If the input cDNA copy number (e.g., volume of cDNA) was within the linear range in samples containing the highest amount of target, then we assumed that it will be linear in samples containing less than the maximum. This assumption holds as long as the change in gene expression was within the dynamic range of the assay. The greatest change in gene expression (Fig. 2) was within the 1-log dynamic range of the endpoint assays (Figs. 4 and 5). The endpoint assays described here introduced greater intraassay variation and produced less linear decay plots than the real-time methods (Tables 2 and 3). However, the endpoint assays may be applied to quantitative mRNA decay studies if access to real-time PCR technology was unavailable.

The levels of β-actin mRNA appear to change during the time course of serum stimulation (Fig. 2). Serum also influenced the expression of three other commonly used housekeeping genes: glyceraldehyde-3-phosphate dehydrogenase, β-2-microglobulin, and 18S rRNA (data not shown). An increase in housekeeping gene expression could be the result of a change in individual mRNA levels or possibly a change in total RNA recovered from the various samples. Future experiments will address this issue.

We demonstrate that real-time quantitative RT-PCR displays a much broader dynamic range and introduces less intraassay variation than endpoint PCR. Comparison of the rank order of the statistical data generated by the linear regression analysis revealed that the real-time methods produced more linear decay plots than the endpoint methods (Table 3). Among the real-time methods, TaqMan and SYBR green produced comparable dynamic range and sensitivity. The SYBR green method was more precise and produced a more linear decay plot than TaqMan detection (Tables 2 and 3). It is difficult to draw broad conclusions about SYBR green and TaqMan quantitative RT-PCR assays based upon the two genes studied here. It is possible that one detection method may be ideal for a particular gene expression experiment or that probe and/or primer optimization may increase assay precision. TaqMan probes have advantages for multiplex assays and add another level of sequence specificity to the PCR. Nonetheless, SYBR green detection represents an economical alternative to TaqMan probes for cDNA measurements in robust PCR systems.

ACKNOWLEDGMENTS

We thank Dr. Jeff Ross for providing us with the 3T3 fos-glo-myc cells and Lori Pritchett and Dr. Mark Tirmenstein for reviewing the manuscript. The technical assistance of Lori Pritchett is greatly appreciated.

REFERENCES

1. Farr, S., and Dunn, R. T., 2nd (1999) Concise review: gene expression applied to toxicology. *Toxicol. Sci.* **50,** 1–9.
2. Zwicker, J., and Muller, R. (1997) Cell-cycle regulation of gene expression by transcriptional repression. *Trends Genet.* **13,** 3–6.
3. Reichel, R. R., and Jacob, S. T. (1993) Control of gene expression by lipophilic hormones. *FASEB J.* **7,** 427–436.

4. Benveniste, E. N. (1997) Cytokines: Influence on glial cell gene expression and function. *Chem. Immunol.* **69,** 31–75.
5. Murphy, L. D., Herzog, C. E., Rudick, J. B., Fojo, A. T., and Bates, S. E. (1990) Use of the polymerase chain reaction in the quantitation of mdr-1 gene expression. *Biochemistry* **29,** 10351–10356.
6. Noonan, K. E., Beck, C., Holzmayer, T. A., Chin, J. E., Wunder, J. S., Andrulis, I. L., Gazdar, A. F., Willman, C. L., Griffith. B., Von-Hoff, D. D., and Robinson, I. B. (1990) Quantitative analysis of MDR1 (multidrug resistance) gene expression in human tumors by polymerase chain reaction. *Proc. Natl. Acad. Sci. USA* **87,** 7160–7164.
7. Dozois, C. M., Oswald, E., Gautier, N., Serthelon, J. P., Fairbrother, J. M., and Oswald, I. P. (1997) A reverse transcription-polymerase chain reaction method to analyze porcine cytokine gene expression. *Vet. Immunol. Immunopathol.* **58,** 287–300.
8. Nakayama, H., Yokoi, H., and Fujita, J. (1992) Quantification of mRNA by non-radioactive RT-PCR and CCD imaging system. *Nucleic Acids Res.* **20,** 4939.
9. Horikoshi, T., Danenberg, K. D., Stadlbauer, T. H., Volkenandt, M., Shea, L. C., Aigner, K., Gustavsson, B., Leichman, L., Frosing, R., Ray, M., *et al.* (1992) Quantitation of thymidylate synthase, dihydrofolate reductase, and DT-diaphorase gene expression in human tumors using the polymerase chain reaction. *Cancer Res.* **52,** 108–116.
10. Guenthner, P. C., and Hart, C. E. (1998) Quantitative, competitive PCR assay for HIV-1 using a microplate-based detection system. *Biotechniques* **24,** 810–816.
11. Heid, C. A., Stevens, J., Livak, K. J., and Williams, P. M. (1996) Real time quantitative PCR. *Genome Res.* **6,** 986–994.
12. Wittwer, C. T., Herrmann, M. G., Moss, A. A., and Rasmussen, R. P. (1997) Continuous fluorescence monitoring of rapid cycle DNA amplification. *Biotechniques* **22,** 130–138.
13. Herrick, D. J., and Ross, J. (1994) The half-life of c-myc mRNA in growing and serum-stimulated cells: Influence of the coding and 3′ untranslated regions and role of ribosome translocation. *Mol. Cell. Biol.* **14,** 2119–28.
14. Kutyavin, I. V., Afonina, I. A., Mills, A. G., Gorn, V., Lukhtanov, E. A., Belousov, E. S., Singer, M. J., Walburger, D., Lokhov, S. G., Gall, A. A., Dempcy, R., Reed, M. W., Meyer, R. B., and Hedgpeth, J. (2000) 3′-Minor groove binder-DNA probes increase sequence specificity at PCR extension temperatures. *Nucleic Acids Res.* **28,** 655–661.
15. Morrison, T. B., Weis, J. J., and Wittwer, C. T. (1998) Quantification of low-copy transcripts by continuous SYBR green I monitoring during amplification. *Biotechniques* **24,** 954–958, 960, 962.
16. Winer, J., Jung, C. K., Shackel, I., and Williams, P. M. (1999) Development and validation of real-time quantitative reverse transcriptase-polymerase chain reaction for monitoring gene expression in cardiac myocytes in vitro. *Anal. Biochem.* **270,** 41–49.
17. Ririe, K. M., Rasmussen, R. P., and Wittwer, C. T. (1997) Product differentiation by analysis of DNA melting curves during the polymerase chain reaction. *Anal. Biochem.* **245,** 154–160.
18. Gerard, C. J., Olsson, K., Ramanathan, R., Reading, C., and Hanania, E. G. (1998) Improved quantitation of minimal residual disease in multiple myeloma using real-time polymerase chain reaction and plasmid-DNA complementarity determining region III standards. *Cancer Res.* **58,** 3957–3964.
19. Pongers-Willemse, M. J., Verhagen, O. J., Tibbe, G. J., Wijkhuijs, A. J., de Haas, V., Roovers, E., van der Schoot, C. E., and van Dongen, J. J. (1988) Real-time quantitative PCR for the detection of minimal residual disease in acute lymphoblastic leukemia using junctional region specific TaqMan probes. *Leukemia* **12,** 2006–2014.
20. Iyer, V. R., Eisen, M. B., Ross, D. T., Schuler, G., Moore, T., Lee, J. C. F., Trent, J. M., Staudt, L. M., Hudson, J., Jr., Boguski, M. S., Lashkari, D., Shalon, D., Botstein, D., and Brown, P. O. (1999) The transcriptional program in the response of human fibroblasts to serum. *Science* **283,** 83–7.
21. Nudel, U., Zakut, R., Shani, M., Neuman, S., Levy, Z., and Yaffe, D. (1983) The nucleotide sequence of the rat cytoplasmic beta-actin gene. *Nucleic Acids Res.* **11,** 1759–1771.